8

Four Exactly Solvable Examples in Non-Equilibrium Thermodynamics of Small Systems

Viktor Holubec, Artem Ryabov, Petr Chvosta
Faculty of Mathematics and Physics, Charles University
V Holešovičkách 2, CZ-180 00 Praha
Czech Republic

1. Introduction

The diffusion dynamics in time-dependent potentials plays a central role in the phenomenon of stochastic resonance (Gammaitoni et al., 1998; Chvosta & Reineker, 2003a; Jung & Hänggi, 1990; 1991), in physics of Brownian motors (Reimann, 2002; Astumian & Hänggi, 2002; Hänggi et al., 2005; Allahverdyan et al., 2008; den Broeck et al., 2004; Sekimoto et al., 2000) and in the discussion concerning the energetics of the diffusion process (Parrondo & de Cisneros, 2002) – these papers discuss history, applications and existing literature in the domain.

Diffusion in a time-dependent potential where the dynamical system communicates with a single thermal bath can be regarded as an example of an isothermal irreversible process. Investigating the work done on the system by the external agent and the heat exchange with the heat bath (Sekimoto, 1999; Takagi & Hondou, 1999) one immediately enters the discussion of the famous Clausius inequality between the irreversible work and the free energy. If the energy considerations concern a small system, the work done on the system has been associated with individual realizations (trajectories) of the diffusive motion, i.e. the work itself is treated as a random variable whose mean value enters the thermodynamic considerations. An important achievement in the field is the discovery of new fluctuation theorems, which generalize the Clausius identity in giving the exact mean value of the exponential of the work. This Jarzynski identity (Bochkov & Kuzovlev, 1981a;b; Evans et al., 1993; Gallavotti & Cohen, 1995; Jarzynski, 1997b;a; Crooks, 1998; 1999; 2000; Maes, 2004; Hatano & Sasa, 2001; Speck & Seifert, 2004; Seifert, 2005; Schuler et al., 2005; Esposito & Mukamel, 2006; Hänggi & Thomas, 1975) enables one to specify the free energy difference between two equilibrium states. This is done by repeating real time (i.e. non-equilibrium) experiment and measuring the work done during the process. The identity has been recently experimentally tested (Mossa et al., 2009; Ritort, 2003).

In the present Chapter we discuss four illustrative, exactly solvable models in non-equilibrium thermodynamics of small systems. The examples concern: i) the *unrestricted* diffusion in the presence of the time-dependent potential (SEC. 2) (Wolf, 1988; Chvosta & Reineker, 2003b; Mazonka & Jarzynski, 1999; Baule & Cohen, 2009; Hänggi & Thomas, 1977), ii) the *restricted* diffusion of non-interacting particles in the presence of the time-dependent potential (SEC. 3) (Chvosta et al., 2005; 2007; Mayr et al., 2007), iii) the restricted diffusion of two *interacting*

particles in the presence of the time-dependent potential (SEC. 4) (Rödenbeck et al., 1998; Lizana & Ambjörnsson, 2009; Kumar, 2008; Ambjörnsson et al., 2008; Ambjörnsson & Silbey, 2008; Barkai & Silbey, 2009), and iv) the two-level system with externally driven energy levels (SEC. 5) (Chvosta et al., 2010; Šubrt & Chvosta, 2007; Henrich et al., 2007; Hänggi & Thomas, 1977).

A common feature of all these examples is the following. Due to the periodic driving, the system approaches a definite steady state exhibiting cyclic energy transformations. The exact solution of underlying dynamical equations allows for the detailed discussion of the limit cycle. Specifically, in the setting i), we present the simultaneous probability density for the particle position and for the work done on the particle. In the model ii), we shall demonstrate that the cycle-averaged spatial distribution of the internal energy differs significantly from the corresponding equilibrium one. In the scenario iii), the particle interaction induces additional entropic repulsive forces and thereby influences the cycle energetics. In the two-level model iv), the system communicates with two heat baths at different temperatures. Hence it can perform a positive mean work per cycle and therefore it can be conceived as a simple microscopic motor. Having calculated the full probability density for the work, we can discuss also fluctuational properties of the motor performance.

2. Diffusion of a particle in a time-dependent parabolic potential

Consider a particle, in contact with a thermal bath at the temperature T which is dragged through the environment by a time-dependent external force. Assuming a single degree of freedom, the location of the particle at a time t is described by the time-inhomogeneous Markov process $\mathsf{X}(t)$. Let the particle moves in the time-dependent potential

$$V(x,t) = \frac{k}{2}[x - u(t)]^2 \,. \tag{1}$$

We can regard the particle as being attached to a spring, the other end of which moves with an instantaneous velocity $\dot{u}(t) \equiv du(t)/dt$. Furthermore, assume that the thermal forces can be modeled as the sum of the linear friction and the Langevin white-noise force. We neglect the inertial forces. Then the equation of motion for the particle position is (van Kampen, 2007):

$$\Gamma \frac{d}{dt}\mathsf{X}(t) = -\frac{\partial}{\partial x}V(x,t)\big|_{x=\mathsf{X}(t)} + \mathsf{N}(t) = -k[\mathsf{X}(t) - u(t)] + \mathsf{N}(t) \,, \tag{2}$$

where Γ is the particle mass times the viscous friction coefficient, and $\mathsf{N}(t)$ represents the delta-correlated white noise $\langle \mathsf{N}(t)\mathsf{N}(t')\rangle = 2D\Gamma^2\,\delta(t-t')$. Here $D = k_{\mathrm{B}}T/\Gamma$ is the diffusion constant and k_{B} is the Boltzmann constant.

We observe the motion of the particle. Assuming a specific trajectory of the particle we are interested in the total work done on the particle if it moves along the trajectory. Taking into account the whole set of all possible trajectories, the work becomes a stochastic process. We denote it as $\mathsf{W}(t)$ and it satisfies the stochastic equation (Sekimoto, 1999)

$$\frac{d}{dt}\mathsf{W}(t) = \frac{\partial}{\partial t}V(\mathsf{X}(t),t) = -k\dot{u}(t)[\mathsf{X}(t) - u(t)] \tag{3}$$

with the initial condition $\mathsf{W}(0) = 0$. Differently speaking, if the particle dwells at the position x during the time interval $[t, t+dt]$ then the work done on the particle during this time interval equals $V(x,t+dt) - V(x,t)$ (for the detailed discussion cf. also SEC. 5).

The above system of stochastic differential equations for the processes $\mathsf{X}(t)$ and $\mathsf{W}(t)$ can be translated into a single partial differential equation for the joint probability density $G(x,w,t\,|\,x_0)$. The function $G(x,w,t\,|\,x_0)$ describes the probability of achieving the position x at the time t *and* performing the work w during the time interval $[0,t]$. The partial differential equation reads (Risken, 1984; van Kampen, 2007)

$$\begin{aligned}\frac{\partial}{\partial t}G(x,w,t\,|\,x_0) = \left\{ D\,\frac{\partial^2}{\partial x^2} + \frac{k}{\Gamma}\frac{\partial}{\partial x}\,[x-u(t)] \;\; + \;\; [x-u(t)]\,\dot{u}(t)\frac{\partial}{\partial w}\right\} G(x,w,t\,|\,x_0)\,,\\ G(x,w,t\,|\,x_0) \;\; = \;\; \delta(x-x_0)\delta(w)\,. \end{aligned} \tag{4}$$

This equation can be solved by several methods. For example, one can use the Lie algebra operator methods (Wilcox, 1967; Wolf, 1988), or one can calculate the joint generating functional for the coupled process in question (Baule & Cohen, 2009). Our approach will be based on the following property of EQ. 4: if at an arbitrary fixed instant the probability density $G(x,w,t\,|\,x_0)$ is of the Gaussian form, then it will preserve this form for all subsequent times. This follows from the fact that all the coefficients on the right hand side of EQ. 4 are polynomials of the degree at most one in the independent variables x and w (van Kampen, 2007). Accordingly, the function $G(x,w,t\,|\,x_0)$ corresponds to a bivariate Gaussian distribution and it is uniquely defined by the central moments (Mazonka & Jarzynski, 1999):

$$\begin{aligned} \overline{x}(t) &= \langle \mathsf{X}(t)\rangle\,, & \overline{w}(t) &= \langle \mathsf{W}(t)\rangle\,,\\ \sigma_x^2(t) &= \left\langle [\mathsf{X}(t)]^2\right\rangle - [\overline{x}(t)]^2\,, & \sigma_w^2(t) &= \left\langle [\mathsf{W}(t)]^2\right\rangle - [\overline{w}(t)]^2\,,\\ c_{xw}(t) &= \langle \mathsf{X}(t)\mathsf{W}(t)\rangle - \overline{x}(t)\overline{w}(t)\,. \end{aligned} \tag{5}$$

The simplest way to calculate these moments is to use EQS. (2) and (3) (Gillespie, 1992; van Kampen, 2007). The result is

$$\overline{x}(t) = u(t) - \exp\left(-\frac{k}{\Gamma}t\right)\int_0^t \mathrm{d}t'\,\dot{u}(t')\exp\left(\frac{k}{\Gamma}t'\right) + [x_0-u(0)]\exp\left(-\frac{k}{\Gamma}t\right), \tag{6}$$

$$\sigma_x^2(t) = \frac{\Gamma D}{k}\left[1-\exp\left(-2\frac{k}{\Gamma}t\right)\right], \tag{7}$$

$$c_{xw}(t) = -2\Gamma D\exp\left(-\frac{k}{\Gamma}t\right)\int_0^t \mathrm{d}t'\,\dot{u}(t')\sinh\left(\frac{k}{\Gamma}t'\right), \tag{8}$$

$$\overline{w}(t) = -k\int_0^t \mathrm{d}t'\,\dot{u}(t')[\overline{x}(t')-u(t')]\,, \qquad \sigma_w^2(t) = -2k\int_0^t \mathrm{d}t'\,\dot{u}(t')c_{xw}(t')\,. \tag{9}$$

Surprisingly, the variance $\sigma_x^2(t)$ does not depend on the function $u(t)$. Moreover, in the asymptotic regime $t \gg \Gamma/k$, the variance $\sigma_x^2(t)$ attains the saturated value $\Gamma D/k$. This means that the marginal probability density for the particle position assumes a time-independent shape.

Up to now our considerations were valid for an arbitrary form of the function $u(t)$. We now focus on the piecewise linear periodic driving. We take $u(t+\lambda) = u(t)$ and

$$u(t) = -2vt \quad \text{for} \quad t\in[0,\tau[\,, \qquad u(t) = -2v\tau + vt \quad \text{for} \quad t\in[\tau,\lambda[\,, \tag{10}$$

where $v>0$ and $0<\tau<\lambda$. The parabola is first moving to the left with the velocity $2v$ during the time interval $[0,\tau[$. Then, at the time τ it changes abruptly its velocity and moves to the right with the velocity v during the rest of the period λ, cf. FIG. 1 d).

Due to the periodic driving the system's response (6)-(9) approaches the limit cycle. FIG. 1 illustrates the response during two such limit cycles. First, note that the mean position of the particle $\overline{x}(t)$ "lags behind" the minimum of the potential well $u(t)$ (see the panel a)). The magnitude of this phase shift is given by the second term in EQ. (6) and therefore it is proportional to the velocity v. In the adiabatic limit of the infinitely slow velocity $v \to 0$ the probability distribution for the particle position is centred at the instantaneous minimum of the parabola.

Consider now the mean work done on the system by the external agent during the time interval $[0,t[$ (panel b)). $\overline{w}(t)$ increases if either simultaneously $u(t) > \overline{x}(t)$ and $\dot{u}(t) > 0$, or if simultaneously $u(t) < \overline{x}(t)$ and $\dot{u}(t) < 0$. For instance, assume the parabola moves to the right and, at the same time, the probability packet for the particle coordinate is concentrated on the left from the instantaneous position of the parabola minimum $u(t)$. Then the dragging rises the potential energy of the particle, i.e. the work is done on it and the mean input power is positive. Similar reasoning holds if either simultaneously $u(t) > \overline{x}(t)$ and $\dot{u}(t) < 0$, or if simultaneously $u(t) < \overline{x}(t)$ and $\dot{u}(t) > 0$. Then the mean work $\overline{w}(t)$ decreases and hence the mean input power is negative. The magnitude of the instantaneous input power is proportional to the instantaneous velocity $\dot{u}(t)$. Therefore it is bigger during the first part of the period of the limit cycle in comparison with the second part of the period. Finally, let us stress that the mean work per cycle $w_{\mathrm{p}} = \overline{w}(t+\lambda) - \overline{w}(t)$ is always positive, as required by the second law of thermodynamics.

The variance of the work done on the particle by the external agent $\sigma_w^2(t)$ shows qualitatively the same behaviour as $\overline{w}(t)$.

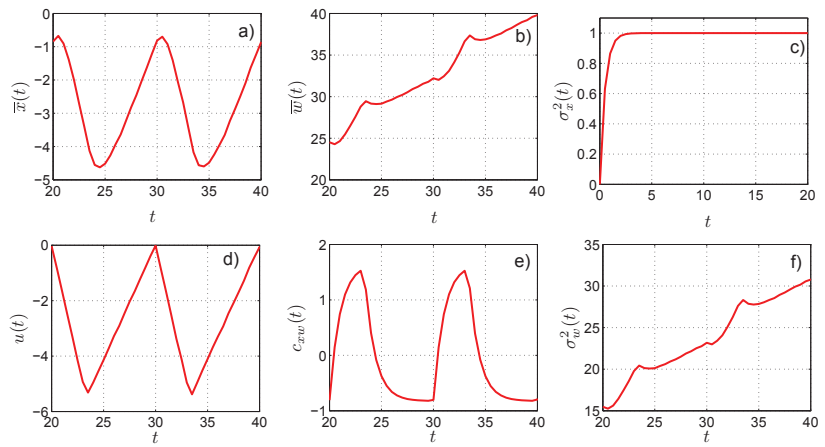

Fig. 1. The central moments (6)-(9) in the time-asymptotic regime. The driving is represented by the position of the potential minimum $u(t)$ and it is depicted in the panel d). In all panels (except of the panel c)) the curves are plotted for two periods λ of the driving. The panel a) shows the mean position of the particle, $\overline{x}(t)$, which lags behind the minimum of the potential well. The panel b) shows the mean work $\overline{w}(t)$ done on the particle by the external agent. In the panel c) we observe the saturation of the variance of the particle's position $\sigma_x^2(t)$. In the panel e) we present the correlation function $c_{xw}(t)$. The panel f) illustrates the variance $\sigma_w^2(t)$ of the work done on the particle by the external agent. The parameters used are: $k = 1\,\mathrm{kg\,s^{-2}}$, $D = 1\,\mathrm{m^2\,s^{-1}}$, $\Gamma = 1\,\mathrm{kg\,s^{-1}}$, $v = 0.825\,\mathrm{m\,s^{-1}}$, $\lambda = 10\,\mathrm{s}$, $\tau = 10/3\,\mathrm{s}$.

3. Barometric process with time-dependent force

3.1 Dynamics

In this Section we discuss a spatially restricted one-dimensional diffusion process occurring in a half-space under the influence of a harmonically oscillating and space-homogeneous driving force. We are interested in the solution of the Langevin equation

$$\Gamma \frac{d}{dt}\mathsf{X}(t) = -\frac{\partial}{\partial x}V(x,t)\big|_{x=\mathsf{X}(t)} + \mathsf{N}(t)\,, \tag{11}$$

for an overdamped Brownian particle moving in the time-dependent potential $V(x,t)$, where $V(x,t) = -xF(t)$, if $x \geq 0$, and $V(x,t) = \infty$, for $x < 0$. Here $\mathsf{N}(t)$ is the δ-correlated Langevin force, and Γ equals the particle mass times the viscous friction coefficient. Differently speaking, while localised on the positive half-line, the particle is acted upon by the Langevin force $\mathsf{N}(t)$ and by the spatially-homogeneous, time-dependent force $F(t)$. Additionally, we assume a reflecting barrier at the origin, i.e. the diffusion is restricted on the positive half-line. As an auxiliary problem, consider first the *spatially unrestricted* one-dimensional diffusion in the field of a spatially-homogeneous and time-dependent force $F(t)$. The probability density for the position of the diffusing particle reads (Hänggi & Thomas, 1975; 1977; Wolf, 1988)

$$G(x,t|x',t') = \frac{1}{\sqrt{\pi}}\,\frac{1}{\sqrt{4D(t-t')}}\exp\left\{-\frac{1}{4D(t-t')}\left[x - x' - \int_{t'}^{t} v(t'')\,dt''\right]^2\right\}. \tag{12}$$

The Green function yields the solution of the Smoluchowski diffusion equation for the initial condition $\pi(x) = \delta(x - x')$ imposed at time t'. Qualitatively, it represents the gradually spreading Gaussian curve whose centre moves in time, the drift being controlled by the protocol (time-dependent scenario) of the external force. The momentary value of the mean particle position is given by the expression $x' + \int_{t'}^{t} ds\, v(s)$, where $v(t) = F(t)/\Gamma$ is the time-dependent drift velocity. The spreading of the Gaussian curve is controlled by the thermal-noise strength parameter $D = k_{\mathrm{B}}T/\Gamma$.

We now assume that the particle is initially (i.e. at the time zero) fully localised at a fixed point $x' > 0$, and we place at the origin of the coordinate system the reflecting boundary. The Green function $U(x,t|x',0)$ which solves the problem with the reflecting boundary can be constructed in two steps (cf. the detailed derivation in Ref. (Chvosta et al., 2005)). First, one has to solve the Volterra integral equation of the first kind

$$D\int_0^t G(0,t|0,t')\,U(0,t'|x',0)\,dt' = \int_{-\infty}^{0} G(x,t|x',0)\,dx\,. \tag{13}$$

Here both the kernel and the right hand side follow directly from Eq. (12). The unknown function $U(0,t|x',0)$ represents, as the designation suggests, the time evolution of the probability density for the restricted diffusion at the boundary. Secondly, the final space-resolved solution emerges after performing just one additional quadrature:

$$U(x,t|x',0) = G(x,t|x',0) - D\int_0^t \frac{\partial}{\partial x}G(x,t|0,t')\,U(0,t'|x',0)\,dt'\,. \tag{14}$$

The resulting function is properly normalized, i.e. we have $\int_0^\infty U(x,t|x',0)\,dx = 1$ for any $t \geq 0$ and for any fixed initial position $x' > 0$.

Up to now, our reasoning is valid for any form of the external driving force. A negative instantaneous force pushes the particle to the left, i.e. against the reflecting boundary at the

origin. In this case, the force acts against the general spreading tendency stemming from the thermal Langevin force. A positive instantaneous force amplifies the diffusion in driving the particle to the right. We now restrict our attention to the case of a harmonically oscillating driving force $F(t) = \Gamma v(t)$ with the drift velocity $v(t) = v_0 + v_1 \sin(\omega t)$. The three parameters, v_0, v_1, and ω occurring in this formula together with the diffusion constant D yield the full description of our setting. Specifically, if $v_1 = 0$, the external force has only the static component and the explicit solution of the integral equation (13) is well known, cf. the formula (29) in (Chvosta et al., 2005). $U(0,t|x',0)$ approaches in this case either zero, if $v_0 \geq 0$, or the value $|v_0|/D$, if $v_0 < 0$. Having the oscillating force, the most interesting physics emerges if the symmetrically oscillating component superposes with a *negative* static force, i.e. if $v_1 > 0$, and $v_0 < 0$. This case is treated in the rest of the Section.

Considering the integral equation (13), the basic difficulty is related with the non-convolution structure of the integral on the left-hand side. It may appear that any attempt to perform the Laplace transformation must fail. But it has been demonstrated in REF. (Chvosta et al., 2007) that this need not be the case. The paper introduces, in full details, a special procedure which yields the exact time-asymptotic solution of EQ. (13). Here we confine ourselves to the statement of the final result and to its physical consequences.

First of all, we introduce an appropriate scaling of the time variable. Adopting any such scaling, the four model parameters will form certain dimensionless groups. However, there are just two "master" combinations of the parameters which control the substantial features of the long-time asymptotic solution. These combinations emerge after we introduce the dimensionless time $\tau = [v_0^2/(4D)]\, t$ (we assume $D > 0$). If we insert the scaled time into EQ. (12), the exponent will include solely the combinations $\kappa = |v_0| v_1 /(2\omega D)$ and $\theta = 4\omega D / v_0^2$. The first of them measures the scaled amplitude of the oscillating force, the second one its scaled frequency. We now define an infinite matrix $\mathbb{R}_{-+}$ with the matrix elements

$$\langle\, m \,|\, \mathbb{R}_{-+} \,|\, n \,\rangle = \mathrm{I}_{|m-n|}(-\kappa\sqrt{1 - \mathrm{i}m\theta} + \kappa)\,. \tag{15}$$

Here m,n are integers and $\mathrm{I}_k(z)$ is the modified Bessel function of order k with argument z. We use the standard bra-ket notation. Notice that the matrix elements depend solely on the above dimensionless combinations κ and θ. As shown in REF. (Chvosta et al., 2005), the time-asymptotic dynamics can be constructed from the matrix elements of the inverse matrix $\mathbb{R}_{-+}^{-1}$. In fact, the so called *complex amplitudes*

$$f_k = \langle\, k \,|\, \mathbb{R}_{-+}^{-1} \,|\, 0 \,\rangle\,,\ k = 0, \pm 1, \pm 2, \ldots\,, \tag{16}$$

define through EQ. (17) below the full solution. The zeroth complex amplitude f_0 equals one. The amplitudes f_k and f_{-k} are complex conjugated numbers. Generally, their absolute value $|f_k|$ decreases with increasing the index k. The even (odd) amplitudes are even (odd) in the parameter κ. Summing up the whole procedure, the probability density at the origin $U(0,t|x',0)$ asymptotically approaches the function

$$U_{\mathrm{a}}(0,t) = \frac{|v_0|}{D} \sum_{k=-\infty}^{+\infty} f_k \exp(-\mathrm{i}k\theta\tau) = \frac{|v_0|}{D} \left\{ 1 + 2 \sum_{k=1}^{\infty} a_k(\kappa,\theta) \cos\left[k\omega t + \phi_k(\kappa,\theta)\right] \right\}. \tag{17}$$

In the last expression, we have introduced the real amplitudes of the higher harmonics $a_k(\kappa,\theta) = |f_k|$ and the phase shifts $\phi_k(\kappa,\theta) = -\arctan(\mathrm{Im}\, f_k / \mathrm{Re}\, f_k)$. Except for the multiplicative factor $|v_0|/D$, the asymptotic form of the probability density at the boundary is

controlled solely by the parameters κ and θ. For example, changing the diffusion constant D and, at the same time, keeping a constant value of the product $D\omega$, the time-asymptotic form of the reduced function $f_a(t) = (D/|v_0|)U_a(0,t)$ will not change. Notice that, for any value of the parameters κ and θ, the time average of the probability density at the boundary equals the equilibrium value of this quantity in the problem without driving force. We have calculated the complex amplitudes (16) via a direct numerical inversion of the matrix $\mathbb{R}_{-+}$ defined in (15). Of course, the infinite-order matrix $\mathbb{R}_{-+}$ must be first reduced onto its finite-order central block. The matrix elements of the reduced matrix are again given by EQ. (15), presently, however, $m,n = 0,\pm1,\pm2,\ldots,\pm N$. The integer N has been taken large enough such that its further increase doesn't change the results, within a predefined precision. In this sense, the numerical results below represent the exact long-time solution of the problem in question.

Up to now, we have only discussed the time-dependence of the probability density at the boundary. As a matter of fact, the knowledge of the complex amplitudes f_k allows for a rather detailed discussion of many other features of the emerging diffusion process. First of all, we focus on the time- and space-resolved probability density for the particle coordinate. We remind that, regardless of the initial condition, the static drift towards the origin ($v_0 < 0$, $v_1 = 0$) induces the unique equilibrium density $\pi_{eq}(x) = (|v_0|/D)\exp[-x|v_0|/D]$, $x \geq 0$. Assuming the oscillating drift, we are again primarily interested in the time-asymptotic dynamics. In this regime, the probability density $U(x,t|x',0)$ does not depend on the initial condition (as represented by the variable x'), and it exhibits at any fixed point $x \geq 0$ oscillations with the fundamental frequency ω. We can write

$$U(x,t|x',0) \sim U_a(x,t) = \sum_{k=-\infty}^{+\infty} u_k(x)\exp(-ik\omega t)\,. \tag{18}$$

Presently, however, the Fourier coefficients $u_k(x)$ depend on the coordinate x. An interesting quantity will be the time-averaged value of the density in the asymptotic regime. This is simply the dc component $u_0(x)$ of the above series. We already know that the value of this function at the origin is $u_0(0) = |v_0|/D$, i.e. it equals the value of the equilibrium density in the static case at the origin, $u_0(0) = \pi_{eq}(0)$. Generically, we call the difference between the time-averaged value of a quantity in the oscillating-drift problem and the corresponding equilibrium value of this quantity in the static case as "dynamical shift". Hence we conclude that there is no dynamical shift of the density profile at the origin. But what happens for $x > 0$? Assume that the complex amplitudes f_k are known. Then we know also the time-asymptotic solution of the integral equation (13) and the subsequent asymptotic analysis can be based on the expression (14). Leaving out the details (cf. again REF. (Chvosta et al., 2007)), the x-dependent Fourier coefficients in EQ. (18) are given by the expression

$$u_k(x) = \frac{|v_0|}{D}\,\langle k|\,\mathbb{L}_{--}\,\mathbb{E}(x)\,\mathbb{R}_{++}\,|\,\mathbf{f}\rangle\,,\ k = 0,\pm1,\pm2,\ldots\,. \tag{19}$$

Here $|\,\mathbf{f}\rangle$ is the column vector of the complex amplitudes, i.e. $f_k = \langle k|\,\mathbf{f}\rangle$. Moreover, we have introduced the diagonal matrix $\mathbb{E}(x)$, and the two matrixes $\mathbb{L}_{--}$, $\mathbb{R}_{++}$ with the matrix

elements

$$\langle m\,|\,\mathbb{E}(x)\,|\,n\rangle \;=\; \frac{\delta_{mn}}{2}\left[1+\frac{1}{\sqrt{1-\mathrm{i}m\theta}}\right]\exp\left[-x\frac{|v_0|}{2D}\left(\sqrt{1-\mathrm{i}m\theta}+1\right)\right], \tag{20}$$

$$\langle m\,|\,\mathbb{L}_{--}\,|\,n\rangle \;=\; \mathrm{I}_{|m-n|}(-\kappa\sqrt{1-\mathrm{i}n\theta}-\kappa)\,, \tag{21}$$

$$\langle m\,|\,\mathbb{R}_{++}\,|\,n\rangle \;=\; \mathrm{I}_{|m-n|}(+\kappa\sqrt{1-\mathrm{i}m\theta}+\kappa)\,, \tag{22}$$

where m and n are integers. FIG. 2 illustrates the time-asymptotic density within two periods of the external driving. Surprising features emerge provided both $\kappa \ll 1$, and $\theta \gg 1$. Under these conditions, the time-averaged probability density $u_0(x)$ exhibits in the vicinity of the boundary a strong dependence on the x-coordinate. It can even develop a well pronounced minimum close to the boundary and, simultaneously, a well pronounced maximum localized farther from the boundary. In between the two extreme values, there exists a spatial region where the time-averaged gradient of the concentration points *against* the time-averaged force. The situation is depicted in FIG. 3 where we have used the same parameters as in FIG. 2. Notice the *positive* dynamical shift $\sigma = \mu_0 - \mu_{\mathrm{eq}}$ of the mean coordinate. Here μ_0 is the

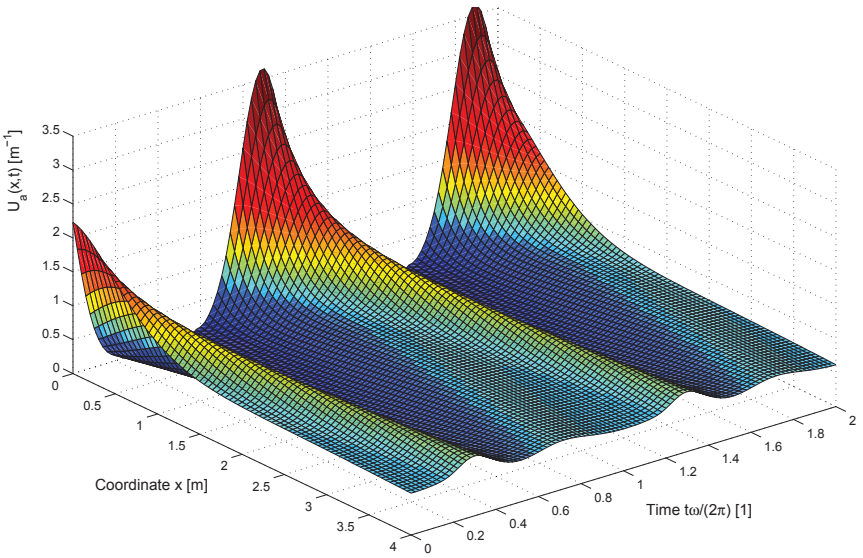

Fig. 2. Time- and space-resolved probability density in the time-asymptotic regime. For any fixed x, the function $U_{\mathrm{a}}(x,t)$ is a periodic function, the period being $2\pi/\omega$. We have plotted it for two periods. The parameters used are: $v_0 = -0.1\,\mathrm{m\,s^{-1}}$, $v_1 = 4.0\,\mathrm{m\,s^{-1}}$, $\omega = 2.0\,\mathrm{rad\,s^{-1}}$, and $D = 1.0\,\mathrm{m^2\,s^{-1}}$. These parameters yield the values $\kappa = 0.1$ and $\theta = 800$.

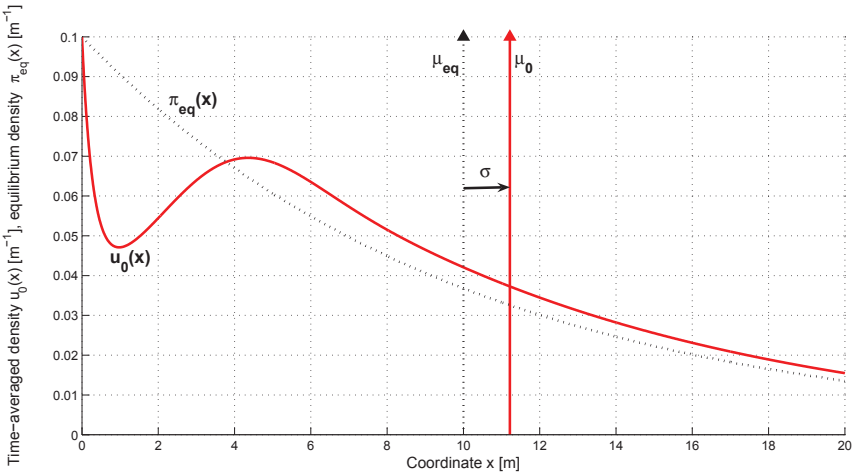

Fig. 3. Time-averaged value $u_0(x)$ of the probability density as the function of the coordinate x. We have used the same set of parameters as in FIG. 2. For comparison, we give also the equilibrium probability density $\pi_{\rm eq}(x) = (|v_0|/D)\exp[-x|v_0|/D]$, $x \geq 0$, in the corresponding static problem. The arrows mark the time-averaged mean position μ_0 in the oscillating-force problem, and the equilibrium mean position in the static problem $\mu_{\rm eq} = D/|v_0|$. Their difference $\sigma = \mu_0 - \mu_{\rm eq}$ represents the dynamical shift of the mean position.

time-averaged mean coordinate

$$\mu_0 = \lim_{t\to\infty} \frac{\omega}{2\pi} \int_t^{t+2\pi/\omega} dt'\, \mu(t',x') \;, \qquad \mu(t,x') = \int_0^\infty dx\, x\, U(x,t|x',0) \;. \tag{23}$$

The exact value of the shift is determined by the complex amplitude f_1 (Chvosta et al., 2007) through $\sigma = (v_1/\omega)\,{\rm Re} f_1$. The small-$v_1$ expansion of the dynamical shift starts with the term v_1^2, i.e. it cannot be described by a linear response theory. If we plot σ as the function of the temperature $T = D\Gamma/k_{\rm B}$ (Chvosta et al., 2007), it exhibits a resonance-like maximum.
Summarizing, the approach elaborated above yields a rather complete picture of the time-asymptotic motion of the diffusing particle. Depending on its distance from the impenetrable boundary, it exhibits non-harmonic oscillations which can be represented as a linear combination of several higher harmonics. The amplitudes and the phases of the harmonics are strongly sensitive to the distance from the boundary. The calculation does not include any small-parameter expansion.

3.2 Energetics

Assuming again the time-dependent potential $V(x,t) = -x[F_0 + F_1\sin(\omega t)]$, where $F_0 = \Gamma v_0$, $F_1 = \Gamma v_1$, the internal energy

$$E(t,x') = \int_0^\infty dx\, V(x,t)\, U(x,t|x',0) = -\Gamma\,[v_0 + v_1\sin(\omega t)]\,\mu(t,x') \;, \tag{24}$$

asymptotically approaches a x'-independent periodic function, say $E_{\rm a}(t)$. In this time-asymptotic regime, the system exhibits periodic changes of its state. The work done

on the system during one such cycle equals to the heat dissipated during the period. An interesting quantity is the time-averaged internal energy

$$E_0 = \lim_{t\to\infty} \frac{\omega}{2\pi} \int_t^{t+2\pi/\omega} dt'\, E(t',x') \,. \tag{25}$$

We can show that E_0 is *always* bigger than the equilibrium internal energy $E_{\rm eq} = D\Gamma = k_{\rm B}T$ in the static problem. Differently speaking, in the time-averaged sense, the external driving enforces a permanent increase of the internal energy, as compared to its equilibrium value.
Having periodic changes of the internal energy, the work done on the system during one period must equal to the heat dissipated during the period. However, their behavior during an infinitesimal time interval within the period is quite different. Generally speaking, the heat ($\equiv$ the dissipated energy) can be identified as the "work" done by the particle on the heat bath (Takagi & Hondou, 1999; Sekimoto, 1999). It arises if and only if the particle moves, i.e. it is inevitable connected with the probability density *current*. More precisely, within our setting, the heat released to the heat bath during the time interval $[0,t]$ is given as

$$Q(t,x') = \int_0^t dt' \int_0^\infty dx \left[-\frac{\partial}{\partial x} V(x,t')\right] J(x,t'|x',0) = \int_0^t dt'\, F(t')\, I(t',x') \,, \tag{26}$$

where $I(t,x') = \int_0^\infty dx\, J(x,t|x',0)$ is the integrated probability current, and $J(x,t|x',0) = \left[v(t) - D\frac{\partial}{\partial x}\right] U(x,t|x',0)$ is the local probability current. The heat released during any infinitesimal time interval is positive. Actually, at any given instant, the force $F(t)$ and the motion of the particle have the same direction. Hence the function which form the integrand in the last expression in EQ. (26) is always nonnegative.
The external agent does work on the system by increasing the potential $V(x,t)$ while the position of the particle is fixed. Thus the work done at a given instant depends on the momentary position of the particle. In the stationary regime, summing over all possible positions *and* over one time period, we get (Chvosta et al., 2005)

$$W = \int_0^{2\pi/\omega} dt' \int_0^\infty dx \left[\frac{\partial}{\partial t'} V(x,t')\right] U_{\rm a}(x,t') = -F_1\omega \int_0^{2\pi/\omega} dt' \cos(\omega t')\, \mu_{\rm a}(t') \,. \tag{27}$$

The work done on the system per cycle equals the area enclosed by the hysteresis curve which represents the parametric plot of the oscillating force versus the mean coordinate in the stationary regime $\mu_{\rm a}(t)$. This quantity must be positive. Otherwise, the system in contact with the single heat bath would produce positive work on the environment during the cyclic process in question. On the other hand, the work done on the system during a definite time interval within the period can be both positive and negative. In order to be specific, let $W_{\rm a}^{(i)}$, $i = 1,\ldots,4$, denote the work done by the external field on the system during the ith quarter-period of the force modulation. During the first quarter-period the slope of the potential decreases and the particle does a positive work on the environment, irrespective to its momentary position. Thus we have $W_{\rm a}^{(1)} < 0$. Nevertheless, the farther is the particle from the boundary the bigger is the work done by it during the fixed time interval. Within the second and the third quarter-period, the slope of the potential increases and the positive work is done by the external agent. Hence we have $W_{\rm a}^{(2)} > 0$ and $W_{\rm a}^{(3)} > 0$. However $W_{\rm a}^{(2)}$ is bigger than $|W_{\rm a}^{(1)}|$, since during the second quarter-period, when the work $W_{\rm a}^{(2)} > 0$ is done, the mean distance of the particle from the boundary is bigger than it was during the first

quarter-period. Similar reasoning holds for the comparison of the work done by the external agent during the third and the fourth quarter-period. We have $W_{\mathrm{a}}^{(4)} < 0$, and $W_{\mathrm{a}}^{(3)} > |W_{\mathrm{a}}^{(4)}|$. On the whole, since the periodic changes of the potential are inevitably associated with the changes of the particle position, the time-averaged work done by the external agent during one fundamental period must be always positive.

4. Two interacting particles in time-dependent potential

Up to now, we have been discussing the diffusion dynamics of just one isolated Brownian particle. Let us now turn to the case of *two interacting* particles diffusing under the action of the time-dependent external force in a one-dimensional channel.

In order to incorporate the simplest inter-particle interaction, the particles can be represented as rods of the length l. *The hard-core interaction* in such system means that the space occupied by one rod is inaccessible to the neighbouring rods. Generally, the diffusion of hard rods can be mapped exactly onto the diffusion of *point particles* (particles with the linear size $l = 0$) by the simple rescaling of space variables (see e.g. (Lizana & Ambjörnsson, 2009)). Hence without loss of generality all further considerations will be done for systems of point particles.

Consider two identical hard-core interacting particles, each with the diffusion constant D, diffusing in the potential $V(x,t)$ (cf. the preceding Section). Due to the hard-core interaction, *particles cannot pass each other* and the ordering of the particles is preserved during the evolution. Starting with $y_1 < y_2$, we have

$$-\infty < \mathsf{X}_1(t) < \mathsf{X}_2(t) < +\infty \tag{28}$$

for any t. We shall call the particle with the coordinate $\mathsf{X}_1(t)$ ($\mathsf{X}_2(t)$) the left (right) one. If the instantaneous coordinates of the two particles differ ($x_1 \neq x_2$) they both diffuse as non-interacting ones. This enables to reduce the diffusion problem for two identical hard-core interacting particles onto the diffusion of one "representative" particle in the two-dimensional *half-plane* $x_1 < x_2$. Namely, it suffices to require that the probability current for this representative particle in the direction perpendicular to the line $x_1 = x_2$ vanishes at this line. Except of that, the dynamics of the representative particle inside the half-plane $x_1 < x_2$ is controlled by the Smoluchowski equation

$$\frac{\partial}{\partial t} p^{(2)}(x_1,x_2,t\,|\,y_1,y_2,t_0) = -\sum_{j=1}^{2} \frac{\partial}{\partial x_j} \left\{ v(t) - D\frac{\partial}{\partial x_j} \right\} p^{(2)}(x_1,x_2,t\,|\,y_1,y_2,t_0)\,. \tag{29}$$

Differently speaking, the hard-core interaction is implemented as the boundary condition

$$\left(\frac{\partial}{\partial x_2} - \frac{\partial}{\partial x_1} \right) p^{(2)}(x_1,x_2,t\,|\,y_1,y_2,t_0)\Big|_{x_1=x_2} = 0\,. \tag{30}$$

Returning to the original picture, *the two hard-core interacting particles in one dimension will never cross each other*.

Assuming the initial positions $y_1 < y_2$, consider the function which is defined as

$$\begin{aligned} p^{(2)}(x_1,x_2,t\,|\,y_1,y_2,t_0) = U(x_1,t\,|\,y_1,t_0)U(x_2,t\,|\,y_2,t_0) + \\ +U(x_1,t\,|\,y_2,t_0)U(x_2,t\,|\,y_1,t_0)\,, \end{aligned} \tag{31}$$

within the phase space $\mathcal{R}_2 : -\infty < x_1 < x_2 < +\infty$, and which vanishes elsewhere. Here $U(x,t\,|\,y,t_0)$ is the solution of the corresponding single-particle problem. This function fulfills

both EQ. (29) and EQ. (30). The proof is straightforward and it can be generalized to the N-particle diffusion problem in a general time- and space-dependent external potential.

4.1 Dynamics

Similarly as in the preceding Section, we now assume the particles are driven by the space-homogeneous and time-dependent force $F(t) = F_0 + F_1 \sin(\omega t)$. The corresponding drift velocity is $v(t) = v_0 + v_1 \sin(\omega t)$ (cf. the preceding Section). The time-independent component pushes the particles to the left against the reflecting boundary at the origin (if $F_0 < 0$), or to the right (if $F_0 > 0$). The time-dependent component $F_1 \sin(\omega t)$ harmonically oscillates with the angular frequency ω. In the rest of this Section we treat the case $F_0 < 0$. On the whole our model includes four parameters F_0, F_1, ω, and D. Notice that the hard-core interaction among particles acts as a purely geometric restriction. As such, it is not connected with any "interaction parameter".

If we integrate the joint probability density (31) over the coordinate x_1 (x_2) of the left (right) particle we obtain the marginal probability density describing the dynamics of the right (left) particle:

$$p_{\mathrm{L}}(x,t\,|\,y_1,y_2,t_0) \equiv \int_0^{+\infty} \mathrm{d}x_2\, p^{(2)}(x,x_2,t\,|\,y_1,y_2,t_0)\,, \tag{32}$$

$$p_{\mathrm{R}}(x,t\,|\,y_1,y_2,t_0) \equiv \int_0^{+\infty} \mathrm{d}x_1\, p^{(2)}(x_1,x,t\,|\,y_1,y_2,t_0)\,. \tag{33}$$

Notice that the both marginal densities depend on the initial positions of the *both* particles. Of course, this is the direct consequence of the interaction among the particles.

Let us now focus on the time-asymptotic dynamics which, as usually, includes the most important physics in the problem. If $F_0 < 0$ and $F_1 = 0$, the probability density of the single diffusing particle relaxes to the exponential function $\pi_{\mathrm{eq}}(x)$ (cf. FIG. 3). Using EQ. (31), the equilibrium two-particle joint probability density is

$$p^{(2)}_{\mathrm{eq}}(x_1,x_2) = \theta(x_2 - x_1) \left(\frac{|v_0|}{D}\right)^2 \exp\left[-(x_1 + x_2)\frac{|v_0|}{D}\right]. \tag{34}$$

Hence the equilibrium probability density of the left particle reads

$$p^{(\mathrm{eq})}_{\mathrm{L}}(x) = 2\theta(x)\frac{|v_0|}{D}\exp\left(-2x\frac{|v_0|}{D}\right). \tag{35}$$

The only difference between this density and $\pi_{\mathrm{eq}}(x)$ is the factor "2" which occurs in the above exponential and as the multiplicative prefactor. Thus $p^{(\mathrm{eq})}_{\mathrm{L}}(x)$ takes a higher value at the boundary and, as the function of the coordinate x, it decreases more rapidly than the single-particle equilibrium density $\pi_{\mathrm{eq}}(x)$. As for the right particle, its equilibrium density could not be so simply related with $\pi_{\mathrm{eq}}(x)$. It reads

$$p^{(\mathrm{eq})}_{\mathrm{R}}(x) = 2\theta(x)\frac{|v_0|}{D}\exp\left(-x\frac{|v_0|}{D}\right)\left[1 - \exp\left(-x\frac{|v_0|}{D}\right)\right]. \tag{36}$$

Notice that it vanishes at the reflecting boundary and it attains its maximum value $p^{(\mathrm{eq})}_{\mathrm{R}}(x_{\mathrm{m}}) = |v_0|/(2D)$ at the coordinate $x_{\mathrm{m}} = D\log(2)/|v_0|$.

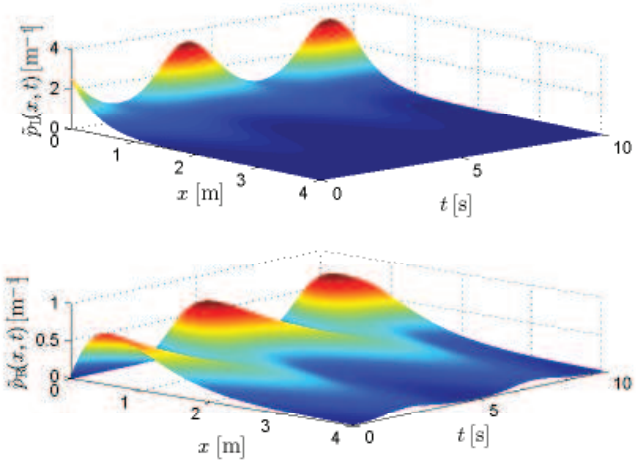

Fig. 4. Time- and space-resolved probability densities in the time-asymptotic regime. We have used the parameters $v_0 = -1.0\,\mathrm{m\,s^{-1}}$, $v_1 = 1.0\,\mathrm{m\,s^{-1}}$, $D = 1.0\,\mathrm{m^2 s^{-1}}$, $\omega = 0.4\,\pi\,\mathrm{rad\,s^{-1}}$.

Let us now take $F_0 < 0$ and $F_1 > 0$. We can simply use the expansion (18) from the preceding Section and insert it into EQ. (31). After this step, the *time-asymptotic* marginal densities (32), (33) read

$$\tilde{p}_L(x,t) = 2\sum_{k=-\infty}^{+\infty}\left[\sum_{n=-\infty}^{+\infty} u_{k-n}(x)\,l_n(x)\right]\exp(-ik\omega t)\,, \tag{37}$$

$$\tilde{p}_R(x,t) = 2\sum_{k=-\infty}^{+\infty}\left[\sum_{n=-\infty}^{+\infty} u_{k-n}(x)\,r_n(x)\right]\exp(-ik\omega t)\,, \tag{38}$$

where we have introduced the abbreviations

$$l_k(x) = \frac{|v_0|}{D}\,\langle k|\,\mathbb{L}_{--}\mathbb{E}_L(x)\mathbb{R}_{++}\,|f\rangle\,, \tag{39}$$

$$r_k(x) = \frac{|v_0|}{D}\,\langle k|\,\mathbb{L}_{--}\mathbb{E}_R(x)\mathbb{R}_{++}\,|f\rangle\,, \tag{40}$$

$$k = 0, \pm 1, \pm 2, \ldots\,.$$

The matrices on the right hand sides are given by EQS. (20)-(22) and by the integrals $\mathbb{E}_L(x) \equiv \int_x^{+\infty} \mathrm{d}x'\mathbb{E}(x')$, $\mathbb{E}_R(x) \equiv \int_0^x \mathrm{d}x'\mathbb{E}(x')$ from the matrix (20).
In order to analyse the densities $\tilde{p}_L(x,t)$ and $\tilde{p}_R(x,t)$ numerically, we have to curtail both the infinite vector of the complex amplitudes $|f\rangle$ and the infinite matrices $\mathbb{L}_{--}$, $\mathbb{R}_{++}$, $\mathbb{E}_L(x)$ and $\mathbb{E}_R(x)$. Using these controllable approximations, we obtain the full time- and space-resolved form of the functions $\tilde{p}_L(x,t)$, $\tilde{p}_R(x,t)$. FIG. 4 illustrates the resulting non-linear "waves".

4.2 Energetics

The equilibrium internal energy of a particle is calculated as the spatial integral from the product of the stationary potential $V(x) = -xF_0$ times the equilibrium probability density. For the single diffusing particle the result is $E^{(\mathrm{eq})} = D\Gamma = k_B T$. In the case of two interacting

particles, the equilibrium internal energy of the left (right) particle reads $E_{\mathrm{L}}^{(\mathrm{eq})} = k_{\mathrm{B}}T/2$ ($E_{\mathrm{R}}^{(\mathrm{eq})} = 3k_{\mathrm{B}}T/2$). The equilibrium internal energies do not depend on the slope of the stationary potential $V(x)$ and they linearly increase with the temperature T. Notice that the effective repulsive force among the interacting particles increases (decreases) the internal energy of the right (left) particle. However, the total internal energy of the system of two interacting particles is equal to the total internal energy of the system of two non-interacting particles, i.e., $E_{\mathrm{L}}^{(\mathrm{eq})} + E_{\mathrm{R}}^{(\mathrm{eq})} = 2E^{(\mathrm{eq})}$. As the hard-core interaction does not contribute to the total energy, the effective repulsive force necessarily arises from a purely entropic effect. This property stems from a zero range of the interaction and it also holds in a general (non-equilibrium) situations.

Now, consider the time-dependent potential $V(x,t) = -xF(t)$. Let the system be in the time-asymptotic regime. The internal energy of the diffusing particle at the time t is defined as the average of the potential $V(x,t)$ over all possible positions of the particle at a given instant. In the single-particle case the internal energy at the time t (say, $E(t)$) is given by EQ. (24). Similarly, in the case of two interacting particles, the internal energies of the left and the right particle are

$$E_{\mathrm{L}}(t) = -[F_0 + F_1 \sin(\omega t)]\mu_{\mathrm{L}}(t)\,, \tag{41}$$

$$E_{\mathrm{R}}(t) = -[F_0 + F_1 \sin(\omega t)]\mu_{\mathrm{R}}(t)\,, \tag{42}$$

respectively. Here, $\mu_{\mathrm{L}}(t)$ ($\mu_{\mathrm{R}}(t)$) denotes the mean position of the left (right) particle in the asymptotic regime.

Generally speaking, the internal energies $E(t)$, $E_{\mathrm{L}}(t)$, $E_{\mathrm{R}}(t)$ are periodic functions of time with the fundamental period $2\pi/\omega$. The total internal energy of two interacting particles is equal

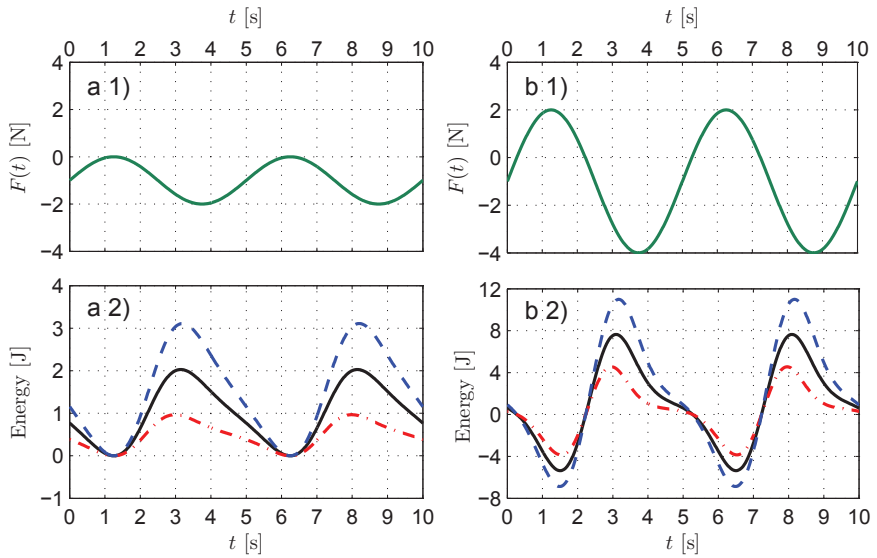

Fig. 5. The internal energies within two periods of the driving. The solid black line shows the energy $E(t)$, the dashed blue line depicts $E_{\mathrm{R}}(t)$ and the dot-dashed red line illustrates $E_{\mathrm{L}}(t)$. In the panels a1) and a2) we take $F_1 = 1.0\,\mathrm{N}$, in the panels b1) and b2) we take $F_1 = 3.0\,\mathrm{N}$. The static component ($F_0 = -1.0\,\mathrm{N}$), the frequency ($\omega = 0.4\,\pi\,\mathrm{s}^{-1}$), and the diffusion constant ($D = 1.0\,\mathrm{m}^2\mathrm{s}^{-1}$) are the same in all panels.

to the total internal energy of two non-interacting particles. In symbols $E_{\mathrm{L}}(t) + E_{\mathrm{R}}(t) = 2E(t)$. FIG. 5 shows the time-dependency of the internal energies $E(t)$, $E_{\mathrm{L}}(t)$, $E_{\mathrm{R}}(t)$ within two periods of the driving force and for the different parameters F_0, F_1, ω, and D. First of all, notice the effect of the entropic repulsive force which stems from the hard-core interaction. We see that there is no *qualitative* difference between the oscillations of the function $E(t)$ and the functions $E_{\mathrm{L}}(t)$, $E_{\mathrm{R}}(t)$. Hence the hard-core interaction changes only *quantitative* features of the energetics of individual particles as compared to the diffusion without interaction. One of this quantitative changes, the most striking one at a first glance, is the change of the amplitudes of the internal energies $E_{\mathrm{L}}(t)$, $E_{\mathrm{R}}(t)$ as compared to $E(t)$.

Oscillations of the internal energies express the combine effect of both the periodically modulated *heat flow* to the bath and the periodic exchange of the *work* done on the particle by an external agent. Without loss of generality let us now analyse the energetics of the single-diffusing particle (solid black lines in FIG. 5). At the beginning of the period we choose the instant when the driving force takes the value F_0 and tends to increase. It is increasing up to the value $F_0 + F_1$. In the panel a 2) $F_0 + F_1 = 0$ N, in the panel b 2) $F_0 + F_1 = 2$ N. During this interval, the internal energy is decreasing towards its minimum due to the positive work which the system does on its surroundings. The smaller the value of the amplitude F_1 (panel a 2)) the closer is the process to the *quasi-static* one and the smaller is the work done by the system. The decreasing tendency of the internal energy is being partially compensated by the heat coming from the heat bath. On the other hand, for larger amplitudes F_1 (panel b 2)), the heat is almost entirely being released to the reservoir. Hence the greater the amplitude F_1 the lower minimum values of the internal energy are observed.

During the next part of the period, the driving force is decreasing form the value $F_0 + F_1$ to its minimum value $F_0 - F_1$. In the panel a 2) $F_0 - F_1 = -2$ N, in the panel b 2) $F_0 - F_1 = -4$ N. Within this interval the slope $-F(t)$ of the potential $V(x,t)$ is permanently increasing, hence the positive work is performed on the system. This work constitutes the most significant contribution to the changes of the internal energy. The internal energy is increasing up to its maximum and, finally, it is decreasing due to the strong heat flow from the system to the bath at the end of this time-interval.

Within the last part of the period, the driving force and the internal energy are decreasing to their initial values which they attain at the beginning of the period. Within this time interval the slope of the potential $V(x,t)$ decreases. Consequently, the positive work is performed by the system on its surrounding. Notice the sudden change of the slope of the internal energy at the beginning of this interval. This effect is more pronounced for the greater amplitudes F_1 (panel b 2)). It is connected with the fact that the system starts to exert work on its surroundings. The greater the amplitude F_1 the less significant the contribution of this work to the change of the internal energy as compared with the heat flow from the system to the reservoir (the more significant contribution of the work would cause faster decreasing of the internal energy as should be seen from the panel a 2)).

Finally let us discus the internal energies averaged over the period, i.e., $\bar{E} = \frac{\omega}{2\pi}\int_0^{2\pi/\omega} \mathrm{d}t E(t)$, $\bar{E}_{\mathrm{L}} = \frac{\omega}{2\pi}\int_0^{2\pi/\omega} \mathrm{d}t E_{\mathrm{L}}(t)$, $\bar{E}_{\mathrm{R}} = \frac{\omega}{2\pi}\int_0^{2\pi/\omega} \mathrm{d}t E_{\mathrm{R}}(t)$. A remarkable fact is that differences $\bar{E} - E^{(\mathrm{eq})}$, $\bar{E}_{\mathrm{L}} - E_{\mathrm{L}}^{(\mathrm{eq})}$, and $\bar{E}_{\mathrm{R}} - E_{\mathrm{R}}^{(\mathrm{eq})}$ are always greater than zero. Differently speaking, in the time-averaged sense, the external driving induces a *permanent increase of the particle's internal energy* as compared to its equilibrium value.

5. Dynamics of a molecular motor based on the externally driven two-level system

Consider a two-level system with time-dependent energies $E_i(t)$, $i = 1,2$, in contact with a single thermal reservoir at temperature T. In general, the heat reservoir temperature T may also be time-dependent. The time evolution of the occupation probabilities $p_i(t)$, $i = 1,2$, is governed by the Master equation (Gammaitoni et al., 1998) with the time-dependent transition rates. The rates depend on the reservoir temperature but they also incorporate external parameters which control the driving protocol. To be specific the dynamics of the system is described by the time-inhomogeneous Markov process $\mathsf{D}(t)$. The state variable $\mathsf{D}(t)$ assumes the value i ($i = 1,2$) if the system resides at the time t in the ith state. Explicitly, the Master equation reads

$$\frac{\mathrm{d}}{\mathrm{d}t}\mathbb{R}(t\,|\,t') = -\begin{pmatrix} \lambda_1(t) & -\lambda_2(t) \\ -\lambda_1(t) & \lambda_2(t) \end{pmatrix}\mathbb{R}(t\,|\,t')\,, \qquad \mathbb{R}(t'\,|\,t') = \mathbb{I}\,, \tag{43}$$

where $\mathbb{I}$ is the unit matrix and $\mathbb{R}(t,t')$ is the transition matrix with the matrix elements $R_{ij}(t\,|\,t') = \langle i\,|\,\mathbb{R}(t\,|\,t')\,|\,j\rangle$. These elements are the conditional probabilities

$$R_{ij}(t\,|\,t') = \mathrm{Prob}\left\{\,\mathsf{D}(t) = i\,|\,\mathsf{D}(t') = j\,\right\}. \tag{44}$$

The occupation probabilities at the observation time t are given by the column vector $|p(t,t')\rangle = \mathbb{R}(t\,|\,t')\,|\phi(t')\rangle$. Here $\phi_i(t') = \langle i\,|\phi(t')\rangle$ denotes the occupational probabilities at the initial time t'. Due to the conservation of the total probability, the system (43) can be reduced to just one non-homogeneous linear differential equation of the first order. Therefore the Master equation (43) is exactly solvable for arbitrary functions $\lambda_1(t)$, $\lambda_2(t)$ (Šubrt & Chvosta, 2007). The rates $\lambda_1(t)$, $\lambda_2(t)$ are typically a product of an attempt frequency ν to exchange the state and an acceptance probability. We shall adopt the Glauber form

$$\lambda_1(t) = \frac{\nu}{1+\exp\left\{-\beta(t)\left[E_1(t)-E_2(t)\right]\right\}},\ \lambda_2(t) = \lambda_1(t)\exp\left\{-\beta(t)\left[E_1(t)-E_2(t)\right]\right\}. \tag{45}$$

Here, ν^{-1} sets the elementary time scale, and $\beta(t) = 1/\left[k_B T(t)\right]$. The rates (45) satisfy the (time local) detailed balance condition (van Kampen, 2007) and they saturate at large energy differences (see (Einax et al., 2010) for a further discussion).

We now introduce the setup for the operational cycle of the engine. Within a given period, two branches with linear time-dependence of the state energies are considered with different velocities. Starting from the value h_1, the energy $E_1(t)$ linearly increases in the first branch until it attains the value $h_2 > h_1$, at the time t_+. Afterwards, in the second branch, the energy $E_1(t)$ linearly decreases and it reassumes the starting value h_1 at the time $t_- + t_+$. We always take $E_2(t) = -E_1(t)$, i.e.

$$E_1(t) = -E_2(t) = \begin{cases} h_1 + \dfrac{h_2-h_1}{t_+}\,t\,, & t \in [0,t_+]\,, \\ h_2 - \dfrac{h_2-h_1}{t_-}\,(t-t_+)\,, & t \in [t_+,t_+ + t_-]\,. \end{cases} \tag{46}$$

This pattern will be periodically repeated, the period being $t_\mathrm{p} = t_+ + t_-$.

As the second ingredient, we need to specify the temperature schedule. The two-level system will be alternately exposed to a hot and a cold reservoir, which means that the function $\beta(t)$ in EQ. (45) will be a piecewise constant periodic function. During the first (second) branch, it assumes the value β_+ (β_-). Let us stress that the change of the heat reservoirs at the end of

the individual branches is instantaneous. The switching of the reservoirs necessarily implies a finite difference between the new reservoir temperature and the actual system (effective) temperature. Even if the driving period tends to infinity (*a quasi-static limit*), we shall observe a positive entropy production originating from the relaxation processes initiated by the abrupt change of the contact temperature. Differently speaking, our engine operates in an inherently irreversible regime and there exists no reversible limit of the limit cycle.
The explicit form of the solution $\mathbb{R}(t\,|\,0)$ of the Master equation (43) with the rates (45) and the periodically modulated energies (46) can be found in (Chvosta et al., 2010). Starting from an arbitrary initial condition $|\phi(t')\rangle$ the system's response approaches a steady state. In order to specify the limit cycle we require that the system's state at the beginning of the cycle coincides with the system state at the end of the cycle. Differently speaking, we have to solve the equation $|\pi\rangle = \mathbb{R}(t_\mathrm{p}\,|\,0)\,|\pi\rangle$ for the unknown initial state $|\pi\rangle$. In the course of the limit cycle, the state of the system is described by the column vector $|p(t)\rangle = \mathbb{R}(t\,|\,0)\,|\pi\rangle$ with the elements $p_i(t) = \langle i\,|\,p(t)\rangle$, $t \in [0, t_\mathrm{p}]$.
This completes the description of the model. Any quantity describing the engine's performance can only depend on the parameters h_1, h_2, $\beta_\pm$, $t_\pm$, and ν.

5.1 Energetics of the engine

During the limit cycle, the internal energy $U(t) = \sum_{i=1}^{2} E_i(t)p_i(t)$ changes as

$$\frac{\mathrm{d}}{\mathrm{d}t}U(t) = \sum_{i=1}^{2} E_i(t)\frac{\mathrm{d}}{\mathrm{d}t}p_i(t) + \sum_{i=1}^{2} p_i(t)\frac{\mathrm{d}}{\mathrm{d}t}E_i(t) = \frac{\mathrm{d}}{\mathrm{d}t}\left[Q(t) + W(t)\right], \quad t \in [0, t_\mathrm{p}]. \tag{47}$$

Here, $Q(t)$ is the mean heat received from the reservoirs during the time interval $[0,t]$. Analogously, $W(t)$ is the mean work done on the system from the beginning of the limit cycle till the time t. If $W(t) < 0$, the positive work $-W(t)$ is done by the system on the environment. Therefore the *oriented* area enclosed by the limit cycle in FIG. 7 represents the work $W_\mathrm{out} \equiv -W(t_\mathrm{p})$ done by the engine on the environment per cycle. This area approaches its maximum absolute value in the quasi-static limit. The internal energy, being a state function, fulfils $U(t_\mathrm{p}) = U(0)$. Therefore, if the work W_out is positive, the same total amount of heat has been accepted from the two reservoirs during the limit cycle. As long as the both heat reservoirs are at the same temperature ($\beta_+ = \beta_-$), the case $W_\mathrm{out} > 0$ will never occur. That the *perpetum mobile* is actually forbidden can be traced back to the detailed balance condition in (43).
We denote the system entropy at the time t as $S_\mathrm{s}(t)$, and the reservoir entropy at the time t as $S_\mathrm{r}(t)$. They are given by

$$\frac{S_\mathrm{s}(t)}{k_\mathrm{B}} = -\left[p_1(t)\ln p_1(t) + p_2(t)\ln p_2(t)\right], \tag{48}$$

$$\frac{S_\mathrm{r}(t)}{k_\mathrm{B}} = \begin{cases} -\beta_+ \displaystyle\int_0^t \mathrm{d}t' E_1(t')\frac{d}{dt'}[p_1(t') - p_2(t')], & t \in [0, t_+], \\ S_\mathrm{r}(t_+) - \beta_- \displaystyle\int_{t_+}^t \mathrm{d}t' E_1(t')\frac{d}{dt'}[p_1(t') - p_2(t')], & t \in [t_+, t_\mathrm{p}]. \end{cases} \tag{49}$$

Upon completing the cycle, the system entropy re-assumes its value at the beginning of the cycle. On the other hand, the reservoir entropy is controlled by the heat exchange. Owing

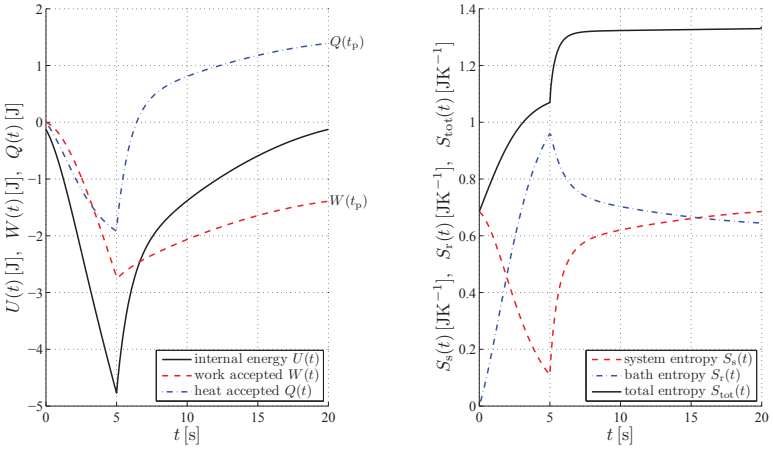

Fig. 6. Thermodynamic quantities as functions of time during the limit cycle. Left panel: internal energy, mean work done on the system, and mean heat received from both reservoirs; the final position of the mean work curve marks the work done on the system per cycle $W(t_p)$. Since $W(t_p) < 0$, the work $W_{out} = -W(t_p)$ has been done on the environment. The internal energy returns to its original value and, after completion of the cycle, the absorbed heat $Q(t_p)$ equals the negative work $-W(t_p)$. Right panel: entropy $S_s(t)$ of the system and $S_r(t)$ of the bath, and their sum $S_{tot}(t)$; after completing the cycle, the system entropy re-assumes its initial value. The difference $S_{tot}(t_p) - S_{tot}(0) > 0$ equals the entropy production per cycle. It is always positive and quantifies the degree of irreversibility of the cycle. Note that at the times t_+ and t_p, strong increase of $S_{tot}(t)$ always occurs due to the instantaneous change of the reservoirs. The parameters used are $h_1 = 1\,\mathrm{J}$, $h_2 = 5\,\mathrm{J}$, $\nu = 1\,\mathrm{s}^{-1}$, $t_+ = 5\,\mathrm{s}$, $t_- = 15\,\mathrm{s}$, $\beta_+ = 0.5\,\mathrm{J}^{-1}$ and $\beta_- = 0.1\,\mathrm{J}^{-1}$.

to the inherent irreversibility of the cycle we observe always a positive entropy production per cycle, i.e., $S_r(t_p) - S_r(0) > 0$. The total entropy $S_{tot}(t) = S_s(t) + S_r(t)$ increases for any $t \in [0, t_p]$. The rate of the increase is the greater the larger is the deviation of the representative point in the $p-E$ diagram from the corresponding equilibrium isotherm (a large deviation, e.g., can be seen in the $p-E$ diagram in FIG. 7 c). Due to the instantaneous exchanges of baths at t_+ and t_p, strong increase of $S_{tot}(t)$ always occurs after these instants. A representative example of the overall behaviour of the thermodynamic quantities (mean work and heat, and entropies) during the limit cycle is shown in FIG. 6.

Up to now, we have discussed the *averaged* thermodynamic properties of the engine. We now turn to the *fluctuations* of its performance.

5.2 Fluctuations of the engine's thermodynamic properties

By treating the state variable and work variable as the two components of a combined stochastic process, it is possible to derive a partial differential equation for the time evolution of the work probability density (or the heat probability density), see, for example, (Schuler et al., 2005; Imparato & Peliti, 2005b;c;a). For completeness, we outline the procedure in the present context.

Heuristically, the underlying time-inhomogeneous Markov process $\mathsf{D}(t)$ can be conceived as an ensemble of individual realizations (sample paths). A realization is specified by a succession of transitions between the two states. If we know the number n of the transitions during a path and the times $t_k{}_{k=1}^{n}$ at which they occur, we can calculate the probability that this specific path will be generated. A given paths yields a unique value of the microscopic work done on the system. For example, if the system is known to remain during the time interval $[t_k, t_{k+1}]$ in the ith state, the work done on the system during this time interval is simply $E_i(t_{k+1}) - E_i(t_k)$. The probability of an arbitrary fixed path amounts, at the same time, the probability of that value of the work which is attributed to the path in question. Viewed in this way, the work itself is a stochastic process and we denote it as $\mathsf{W}(t)$. We are interested in its probability density $\rho(w,t) = \langle \delta(\mathsf{W}(t) - w) \rangle$, where $\langle \ldots \rangle$ denotes the average over all possible paths.

We now introduce the *augmented process* $\{\mathsf{W}(t), \mathsf{D}(t)\}$ which simultaneously reflects both the work variable and the state variable. The augmented process is again a time non-homogeneous Markov process. Actually, if we know at a fixed time t' both the present state variable j and the work variable w', then the subsequent probabilistic evolution of the state and the work is completely determined. The work done during the time period $[t', t]$, where $t > t'$, simply adds to the present work w' and it only depends on the succession of the states after the time t'. And this succession by itself cannot depend on the dynamics before time t'.

The one-time properties of the augmented process will be described by the functions

$$G_{ij}(w,t\,|\,w',t') = \lim_{\epsilon\to 0} \frac{\mathrm{Prob}\,\{\,\mathsf{W}(t) \in (w, w+\epsilon) \,\mathrm{and}\, \mathsf{D}(t) = i \,|\, \mathsf{W}(t') = w' \,\mathrm{and}\, \mathsf{D}(t') = j\,\}}{\epsilon}, \tag{50}$$

where $i, j = 1, 2$. We represent them as the matrix elements of a single two-by-two matrix $\mathbb{G}(w,t\,|\,w',t')$,

$$G_{ij}(w,t\,|\,w',t') = \langle\, i \,|\, \mathbb{G}(w,t\,|\,w',t') \,|\, j \,\rangle\,. \tag{51}$$

We need an equation which controls the time dependence of the propagator $\mathbb{G}(w,t\,|\,w',t')$ and which plays the same role as the Master equation (43) in the case of the simple two-state process. This equation reads (Imparato & Peliti, 2005b; Šubrt & Chvosta, 2007)

$$\frac{\partial}{\partial t}\mathbb{G}(w,t\,|\,w',t') = -\left\{ \begin{pmatrix} \frac{dE_1(t)}{dt} & 0 \\ 0 & \frac{dE_2(t)}{dt} \end{pmatrix} \frac{\partial}{\partial w} + \begin{pmatrix} \lambda_1(t) & -\lambda_2(t) \\ -\lambda_1(t) & \lambda_2(t) \end{pmatrix} \right\} \mathbb{G}(w,t\,|\,w',t'), \tag{52}$$

where the initial condition is $\mathbb{G}(w,t'\,|\,w',t') = \delta(w - w')\mathbb{I}$. The matrix equation represents a hyperbolic system of four coupled partial differential equations with the time-dependent coefficients.

Similar reasoning holds for the random variable $\mathsf{Q}(t)$ which represents the heat accepted by the system from the environment. Concretely, if the system undergoes during a time interval $[t_k, t_{k+1}]$ only one transition which brings it at an instant $\tau \in [t_k, t_{k+1}]$ from the state i to the state j, the heat accepted by the system during this time interval is $E_j(\tau) - E_i(\tau)$. The variable $\mathsf{Q}(t)$ is described by the propagator $\mathbb{K}(q,t\,|\,q',t')$ with the matrix elements

$$K_{ij}(q,t\,|\,q',t') = \lim_{\epsilon\to 0} \frac{\mathrm{Prob}\,\big\{\mathsf{Q}(t) \in (q, q+\epsilon) \,\wedge\, \mathsf{D}(t) = i \,|\, \mathsf{Q}(t') = q' \,\wedge\, \mathsf{D}(t') = j\big\}}{\epsilon}. \tag{53}$$

It turns out that there exists a simple relation between the heat propagator and the work propagator $\mathbb{G}(w,t\,|\,w',t')$. Since for each path, heat q and work w are connected by the first law of thermodynamics, we have $q = E_i(t) - E_j(t') - w$ for any path which has started at the time t' in the state j and which has been found at the time t in the state i. Accordingly,

$$\mathbb{K}(q,t\,|\,q',t') = \begin{pmatrix} g_{11}(u_{11}(t,t') - q, t\,|\,q',t') & g_{12}(u_{12}(t,t') - q, t\,|\,q',t') \\ g_{21}(u_{21}(t,t') - q, t\,|\,q',t') & g_{22}(u_{22}(t,t') - q, t\,|\,q',t') \end{pmatrix}, \tag{54}$$

where $u_{ij}(t,t') = E_i(t) - E_j(t')$.
The explicit form of the matrix $\mathbb{G}(w,t)$ which solves the dynamical equation (52) with the Glauber transition rates (45) and the periodically modulated energies (46) can be found in (Chvosta et al., 2010). Heaving the matrix $\mathbb{G}(w,t)$ for the limit cycle, the matrix $\mathbb{K}(q,t)$ is calculated using the transformation (54).
In the last step, we take into account the initial condition $|\,\pi\,\rangle$ at the beginning of the limit cycle and we sum over the final states of the process $\mathsf{D}(t)$. Then the (unconditioned) probability density for the work done on the system in the course of the limit cycle reads

$$\rho(w,t) = \sum_{i=1}^{2} \langle\, i\,|\,\mathbb{G}(w,t)\,|\,\pi\,\rangle\,. \tag{55}$$

Similarly, the probability density for the heat accepted during the time interval $[0,t]$ is

$$\chi(q,t) = \sum_{i=1}^{2} \langle\, i\,|\,\mathbb{K}(q,t)\,|\,\pi\,\rangle\,. \tag{56}$$

The form of the resulting probability densities and therefore also the overall properties of the engine critically depend on the two dimensionless parameters $a_\pm = \nu t_\pm/(2\beta_\pm|h_2 - h_1|)$. We call them *reversibility parameters* [1]. For a given branch, say the first one, the parameter a_+ represents the ratio of two characteristic time scales. The first one, $1/\nu$, describes the attempt rate of the internal transitions. The second scale is proportional to the reciprocal driving velocity. Contrary to the first scale, the second one is fully under the external control. Moreover, the reversibility parameter a_+ is proportional to the absolute temperature of the heat bath, k_B/β_+.
FIG. 7 illustrates the shape of the limit cycle together with the functions $\rho(w,t_\mathrm{p})$, $\chi(q,t_\mathrm{p})$ for various values of the reversibility parameters. Notice that the both functions $\rho(w,t_\mathrm{p})$ and $\chi(q,t_\mathrm{p})$ vanishes outside a finite support. Within their supports, they exhibit a continuous part, depicted by the full curve, and a singular part, illustrated by the full arrow. The height of the full arrow depicts the weight of the corresponding δ-function. The continuous part of the function $\rho(w,t_\mathrm{p})$ develops one discontinuity which is situated at the position of the full arrow. Similarly, the continuous part of the function $\chi(q,t_\mathrm{p})$ develops three discontinuities.
If the both reversibility parameters $a_\pm$ are small, the isothermal processes during the both branches strongly differ from the equilibrium ones. The indication of this case is a flat continuous component of the density $\rho(w,t_\mathrm{p})$ and a well pronounced singular part. The strongly irreversible dynamics occurs if one or more of the following conditions hold. First, if ν is small, the transitions are rare and the occupation probabilities of the individual energy

[1] The reversibility here refers to the individual branches. As pointed out above, the abrupt change in temperature, when switching between the branches, implies that there exists no reversible limit for the complete cycle.

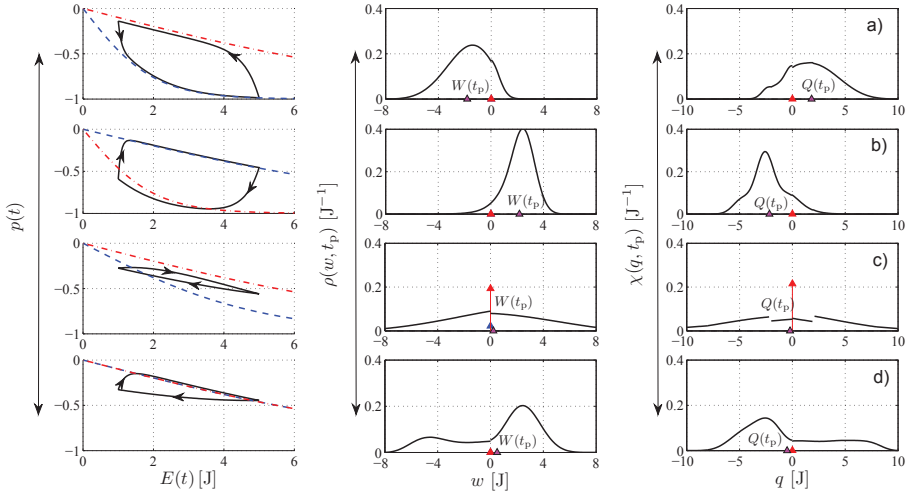

Fig. 7. Probability densities $\rho(w,t_{\rm p})$ and $\chi(q,t_{\rm p})$ for the work and the heat for four representative sets of the engine parameters (every set of parameters corresponds to one horizontal triplet of the panels). The first panel in the triplet shows the limit cycle in the $p-E$ plane ($p(t)=p_1(t)-p_2(t)$ is the occupation difference and $E(t)=E_1(t)$). In the parametric plot we have included also the equilibrium isotherm which corresponds to the first stroke (the dashed line) and to the second stroke (the dot-dashed line). In all panels we take $h_1=1$ J, $h_2=5$ J, and $\nu=1\,{\rm s}^{-1}$. The other parameters are the following. a in the first triplet: $t_+=50$ s, $t_-=10$ s, $\beta_+=0.5\,{\rm J}^{-1}$, $\beta_-=0.1\,{\rm J}^{-1}$, $a_\pm=12.5$ (the bath of the first stroke is colder than that of the second stroke). b in the second triplet: $t_+=50$ s, $t_-=10$ s, $\beta_+=0.1\,{\rm J}^{-1}$, $\beta_-=0.5\,{\rm J}^{-1}$, $a_+=62.5$, $a_-=2.5$ (exchange of β_+ and β_- as compared to case a, leading to a change of the traversing of the cycle from counter-clockwise to clockwise and a sign reversal of the mean values $W(t_{\rm p})\equiv\langle\,{\sf W}(t_{\rm p})\,\rangle$ and $Q(t_{\rm p})\equiv\langle\,{\sf Q}(t_{\rm p})\,\rangle$). c in the third triplet: $t_+=2$ s, $t_-=2$ s, $\beta_+=0.2\,{\rm J}^{-1}$, $\beta_-=0.1\,{\rm J}^{-1}$, $a_+=1.25$, $a_-=2.5$ (a strongly irreversible cycle traversed clockwise with positive work). d in the fourth triplet: $t_+=20$ s, $t_-=1$ s, $\beta_\pm=0.1\,{\rm J}^{-1}$, $a_+=25$, $a_-=1.25$ (no change in temperatures, but large difference in duration of the two strokes; $W(t_{\rm p})$ is necessarily positive). The height of the red arrows plotted in the panels with probability densities depicts the weight of the corresponding δ-functions.

levels are effectively frozen during long periods of time. Therefore they lag behind the Boltzmann distribution which would correspond to the instantaneous positions of the energy levels. More precisely, the population of the ascending (descending) energy level is larger (smaller) than it would be during the corresponding reversible process. As a result, the mean work done on the system is necessarily larger than the equilibrium work. Secondly, a similar situation occurs for large driving velocities $v_\pm$. Due to the rapid motion of the energy levels, the occupation probabilities again lag behind the equilibrium ones. Thirdly, the strong irreversibility occurs also in the low temperature limit. In the limit $a_\pm\to 0$, the continuous part vanishes and $\rho(w,t_{\rm p})=\delta(w)$.

In the opposite case of large reversibility parameters $a_\pm$, the both branches in the $p-E$ plane are located close to the reversible isotherms. The singular part of the density $\rho(w,t_{\rm p})$ is suppressed and the continuous part exhibits a well pronounced peak. The density $\rho(w,t_{\rm p})$ approaches the Gaussian function centered around the men work. This confirms the general

considerations (Speck & Seifert, 2004). In the limit $a_{\pm} \to \infty$ the Gaussian peak collapses to the delta function located at the quasi-static work (Chvosta et al., 2010). The heat probability density $\chi(q, t_{\mathrm{p}})$ shows similar properties as $\rho(w, t_{\mathrm{p}})$.

6. Acknowledgements

Support of this work by the Ministry of Education of the Czech Republic (project No. MSM 0021620835), by the Grant Agency of the Charles University (grant No. 143610) and by the projects SVV – 2010 – 261 301, SVV – 2010 – 261 305 of the Charles University in Prague is gratefully acknowledged.

7. References

Allahverdyan, A. E., Johal, R. S. & Mahler, G. (2008). Work extremum principle: Structure and function of quantum heat engines, *Phys. Rev. E* 77(4): 041118.

Ambjörnsson, T., Lizana, L., Lomholt, M. A. & Silbey, R. J. (2008). Single-file dynamics with different diffusion constants, *J. Chem. Phys.* 129: 185106.

Ambjörnsson, T. & Silbey, R. J. (2008). Diffusion of two particles with a finite interaction potential in one dimension, *J. Chem. Phys.* 129: 165103.

Astumian, R. & Hänggi, P. (2002). Brownian motors, *Phys. Today* 55(11): 33.

Barkai, E. & Silbey, R. J. (2009). Theory of single-file diffusion in a force field, *Phys. Rev. Lett.* 102: 050602.

Baule, A. & Cohen, E. G. D. (2009). Fluctuation properties of an effective nonlinear system subject to Poisson noise, *Phys. Rev. E* 79(3): 030103.

Bochkov, G. N. & Kuzovlev, Y. E. (1981a). Nonlinear fluctuation-dissipation relations and stochastic models in nonequilibrium thermodynamics: I. Generalized fluctuation-dissipation theorem, *Physica A* 106: 443.

Bochkov, G. N. & Kuzovlev, Y. E. (1981b). Nonlinear fluctuation-dissipation relations and stochastic models in nonequilibrium thermodynamics: II. Kinetic potential and variational principles for nonlinear irreversible processes, *Physica A* 106: 480.

Chvosta, P., Einax, M., Holubec, V., Ryabov, A. & Maass, P. (2010). Energetics and performance of a microscopic heat engine based on exact calculations of work and heat distributions, *J. Stat. Mech.* p. P03002.

Chvosta, P. & Reineker, P. (2003a). Analysis of stochastic resonances, *Phys. Rev. E* 68(6): 066109.

Chvosta, P. & Reineker, P. (2003b). Diffusion in a potential with a time-dependent discontinuity, *Journal of Physics A: Mathematical and General* 36(33): 8753.

Chvosta, P., Schulz, M., Mayr, E. & Reineker, P. (2007). Sedimentation of particles acted upon by a vertical, time-oscillating force, *New. J. Phys.* 9: 2.

Chvosta, P., Schulz, M., Paule, E. & Reineker, P. (2005). Kinetics and energetics of reflected diffusion process with time-dependent and space-homogeneous force, *New. J. Phys.* 7: 190.

Crooks, G. E. (1998). Nonequilibrium measurements of free energy differences for microscopically reversible Markovian systems, *J. Stat. Phys.* 90(5–6): 1481–1487.

Crooks, G. E. (1999). Entropy production fluctuation theorem and the nonequilibrium work relation for free energy differences, *Phys. Rev. E* 60(3): 2721–2726.

Crooks, G. E. (2000). Path-ensemble averages in systems driven far from equilibrium, *Phys. Rev. E* 61(3): 2361–2366.

den Broeck, C. V., Kawai, R. & Meurs, P. (2004). Microscopic analysis of a thermal Brownian

motor, *Phys. Rev. Lett.* 93(9): 090601.
Einax, M., Körner, M., Maass, P. & Nitzan, A. (2010). Nonlinear hopping transport in ring systems and open channels, *Phys. Chem. Chem. Phys.* 10: 645–654.
Esposito, M. & Mukamel, S. (2006). Fluctuation theorems for quantum master equations, *Phys. Rev. E* 73(4): 046129.
Evans, D. J., Cohen, E. G. D. & Morriss, G. P. (1993). Probability of second law violations in shearing steady states, *Phys. Rev. Lett.* 71(15): 2401–2404.
Gallavotti, G. & Cohen, E. G. D. (1995). Dynamical ensembles in nonequilibrium statistical mechanics, *Phys. Rev. Lett.* 74(14): 2694–2697.
Gammaitoni, L., Hänggi, P., Jung, P. & Marchesoni, F. (1998). Stochastic resonance, *Rev. Mod. Phys.* 70(1): 223–287.
Gillespie, D. T. (1992). *Markov Processes: an Introduction for Physical Scientists*, San Diego: Academic Press, San Diego.
Hänggi, P., Marchesoni, F. & Nori, F. (2005). Brownian motors, *Ann. Phys.* 14(11): 51–70.
Hänggi, P. & Thomas, H. (1975). Linear response and fluctuation theorems for nonstationary stochastic processes, *Z. Physik B* 22: 295–300.
Hänggi, P. & Thomas, H. (1977). Time evolution, correlations and linear response of non-Markov processes, *Z. Physik B* 26: 85–92.
Hatano, T. & Sasa, S. (2001). Steady-state thermodynamics of Langevin systems, *Phys. Rev. Lett.* 86(16): 3463–3466.
Henrich, M. J., Rempp, F. & Mahler, G. (2007). Quantum thermodynamic Otto machines: A spin-system approach, *Eur. Phys. J. Special Topics* 151: 157–165.
Imparato, A. & Peliti, L. (2005a). Work distribution and path integrals in general mean-field systems, *EPL* 70(6): 740–746.
Imparato, A. & Peliti, L. (2005b). Work probability distribution in single-molecule experiments, *EPL* 69(4): 643–649.
Imparato, A. & Peliti, L. (2005c). Work-probability distribution in systems driven out of equilibrium, *Phys. Rev. E* 72(4): 046114.
Jarzynski, C. (1997a). Equilibrium free-energy differences from nonequilibrium measurements: A master-equation approach, *Phys. Rev. E* 56(5): 5018–5035.
Jarzynski, C. (1997b). Nonequilibrium equality for free energy differences, *Phys. Rev. Lett.* 78(14): 2690–2693.
Jung, P. & Hänggi, P. (1990). Resonantly driven Brownian motion: Basic concepts and exact results, *Phys. Rev. A* 41(6): 2977–2988.
Jung, P. & Hänggi, P. (1991). Amplification of small signals via stochastic resonance, *Phys. Rev. A* 44(12): 8032–8042.
Kumar, D. (2008). Diffusion of interacting particles in one dimension, *Phys. Rev. E* 78: 021133.
Lizana, L. & Ambjörnsson, T. (2009). Diffusion of finite-sized hard-core interacting particles in a one-dimensional box: Tagged particle dynamics, *Phys. Rev. E* 80: 051103.
Maes, C. (2004). On the origin and use of fluctuation relations for the entropy, *in* J. Dalibard, B. Duplantier & V. Rivasseau (eds), *Poincaré Seminar 2003: Bose-Einstein condensation-entropy*, Birkhäuser, Basel, pp. 149–191.
Mayr, E., Schulz, M., Reineker, P., Pletl, T. & Chvosta, P. (2007). Diffusion process with two reflecting barriers in a time-dependent potential, *Phys. Rev. E* 76(1): 011125.
Mazonka, O. & Jarzynski, C. (1999). Exactly solvable model illustrating far-from-equilibrium predictions, *arXiv.org:cond-mat 9912121* .
Mossa, A., M. Manosas, N. F., Huguet, J. M. & Ritort, F. (2009). Dynamic force spectroscopy of

DNA hairpins: I. force kinetics and free energy landscapes, *J. Stat. Mech.* p. P02060.
Parrondo, J. M. R. & de Cisneros, B. J. (2002). Energetics of Brownian motors: a review, *Applied Physics A* 75: 179–191. 10.1007/s003390201332.
Reimann, P. (2002). Brownian motors: noisy transport far from equilibrium, *Phys. Rep.* 361: 57–265.
Risken, H. (1984). *The Fokker-Planck Equation. Methods of Solution and Applications*, Springer-Verlag, Berlin - Heidelberg - New York - Tokyo.
Ritort, F. (2003). Work fluctuations, transient violations of the second law, *Poincaré Seminar 2003: Bose-Einstein condensation-entropy*, Birkhäuser, Basel, pp. 195–229.
Rödenbeck, C., Kärger, J. & Hahn, K. (1998). Calculating exact propagators in single-file systems via the reflection principle, *Phys. Rev. E* 57: 4382.
Schuler, S., Speck, T., Tietz, C., Wrachtrup, J. & Seifert, U. (2005). Experimental test of the fluctuation theorem for a driven two-level system with time-dependent rates, *Phys. Rev. Lett.* 94(18): 180602.
Seifert, U. (2005). Entropy production along a stochastic trajectory and an integral fluctuation theorem, *Phys. Rev. Lett.* 95(4): 040602.
Sekimoto, K. (1999). Kinetic characterization of heat bath and the energetics of thermal ratchet models, *J. Phys. Soc. Jpn.* 66: 1234–1237.
Sekimoto, K., Takagi, F. & Hondou, T. (2000). Carnot's cycle for small systems: Irreversibility and cost of operations, *Phys. Rev. E* 62(6): 7759–7768.
Speck, T. & Seifert, U. (2004). Distribution of work in isothermal nonequilibrium processes, *Phys. Rev. E* 70(6): 066112.
Šubrt, E. & Chvosta, P. (2007). Exact analysis of work fluctuations in two-level systems, *J. Stat. Mech.* p. P09019.
Takagi, F. & Hondou, T. (1999). Thermal noise can facilitate energy conversion by a ratchet system, *Phys. Rev. E* 60(4): 4954–4957.
van Kampen, N. G. (2007). *Stochastic Process in Physics and Chemistry*, Elsevier.
Wilcox, R. M. (1967). Exponential operators and parameter differentiation in quantum physics, *J. Math. Phys.* 8: 962–982.
Wolf, F. (1988). Lie algebraic solutions of linear Fokker-Planck equations, *J. Math. Phys.* 29: 305–307.

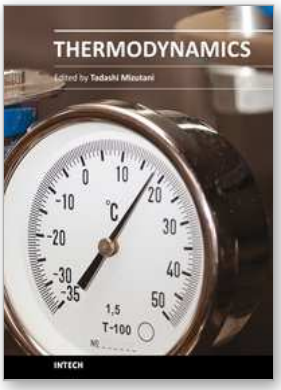

Thermodynamics

Edited by Prof. Mizutani Tadashi

ISBN 978-953-307-544-0

Hard cover, 440 pages

Publisher InTech

Published online 14, January, 2011

Published in print edition January, 2011

Progress of thermodynamics has been stimulated by the findings of a variety of fields of science and technology. The principles of thermodynamics are so general that the application is widespread to such fields as solid state physics, chemistry, biology, astronomical science, materials science, and chemical engineering. The contents of this book should be of help to many scientists and engineers.

How to reference

In order to correctly reference this scholarly work, feel free to copy and paste the following:

Viktor Holubec, Artem Ryabov and Petr Chvosta (2011). Four Exactly Solvable Examples in Non-Equilibrium Thermodynamics of Small Systems, Thermodynamics, Prof. Mizutani Tadashi (Ed.), ISBN: 978-953-307-544-0, InTech, Available from: http://www.intechopen.com/books/thermodynamics/four-exactly-solvable-examples-in-non-equilibrium-thermodynamics-of-small-systems

INTECH
open science | open minds

InTech Europe
University Campus STeP Ri
Slavka Krautzeka 83/A
51000 Rijeka, Croatia
Phone: +385 (51) 770 447
Fax: +385 (51) 686 166
www.intechopen.com

InTech China
Unit 405, Office Block, Hotel Equatorial Shanghai
No.65, Yan An Road (West), Shanghai, 200040, China
中国上海市延安西路65号上海国际贵都大饭店办公楼405单元
Phone: +86-21-62489820
Fax: +86-21-62489821